which is a Gaussian function of φ with a characteristic width $1/F_H$ and a maximum at $\varphi=\frac{T}{F_H}\Delta 2\theta$.

Similar results are obtained for a 2θ scan at constant φ.

θ–2θ Scan

For a θ–2θ scan, $\varphi=\Delta\theta$, so that from equation (40*b*) we have

$$S^2_{\theta,2\theta}=S^2_H(\Delta\theta)^2, \tag{45}$$

where

$$S^2_H=F^2_H+4N^2-4L_S\,. \tag{46}$$

The intensity is therefore given by

$$I_{\theta,2\theta}=I_0\exp\{-\tfrac{1}{2}S^2_H(\Delta\theta)^2\}, \tag{47}$$

which is a Gaussian function of $\Delta\theta$ with characteristic width $1/S_H$.

Orientation of the resolution ellipsoid

The results of the previous sections enable us to determine the size and orientation of the resolution ellipsoid. If we define orthogonal axes as before (paper II) with $\Delta\mathbf{Q}_x$ parallel to $\mathbf{Q}$ and $\Delta\mathbf{Q}_z$ vertical, we can derive the resolution ellipsoid from equations (25), (30), (35) and (47) to be:

$$a\Delta Q^2_x+b\Delta Q^2_y+c\Delta Q^2_z+2h\Delta Q_x\Delta Q_y=1 \tag{48}$$

where

$$a=S^2_H/\cos^2\theta_S \tag{49a}$$

$$b=F^2_H/\sin^2\theta_S \tag{49b}$$

$$c=J^2/\sin^2\theta_S \tag{49c}$$

$$h=(2L_S-F^2_H)/(\sin\theta_S\cos\theta_S) \tag{49d}$$

and the angles μ_2 made by the principal axes to $\mathbf{Q}$ are given by $\tan\mu_2=m_j$ ($j=1$, 2, or 3), where m_1 and m_2 are given by the roots of the equation

$$hm^2+m(a-b)-h=0 \tag{50}$$

and $m_3=\infty$.

References

COOPER, M. J. & NATHANS, R. (1966). *J. Appl. Phys.* **37** 1041.

COOPER, M. J. & NATHANS, R. (1967). *Acta Cryst.* **23**, 357.

COOPER, M. J. & NATHANS, R. (1968). *Acta Cryst.* A**24**, 481.

COOPER, M. J. (1968). A**24**, 624.

Acta Cryst. (1968). A**24**, 624

The Resolution Function in Neutron Diffractometry IV. Application of the Resolution Function to the Measurement of Bragg Peaks*

BY M. J. COOPER†

Materials Physics Division, A.E.R.E., Harwell, Berks., England

(*Received* 6 *June* 1968)

The application of the resolution function of a two-crystal neutron diffractometer to the measurement of Bragg peaks is discussed in detail and experimental measurements of peak widths are compared with theoretical predictions.

1. Introduction

In the previous paper (part III: Cooper & Nathans, 1968) we derived the form of various scans through a Bragg peak for a perfect crystal sample in order to demonstrate the use of experimental Bragg profile measurements in determining the resolution function of a two-crystal neutron diffractometer. In the present paper we shall examine more closely the dependence of these scans on the instrumental parameters, considering such factors as focusing effects, and extend the analysis to the case of Bragg peaks for imperfect single crystals. Experimental results which support this analysis are also given.

2. Crystal (φ) scans

(*a*) *Perfect sample*

The intensity observed when a perfect sample has been rotated through an angle φ from the optimum setting for the measurement of a Bragg reflexion has been derived in equation (25) of paper III. The characteristic width of a φ-scan is $\Phi_0=1/F_H$, where F_H is defined by equation (24*b*) of paper III.

* Work performed in part under the auspices of the U.S. Atomic Energy Commission.

† Formerly Research Associate, Brookhaven National Laboratory, N.Y., U.S.A.

Expanding the expression for F_H^2 we obtain

$$F_H^2=k_I^2\{[A_1^2+A_2^2]\,[(H_M+C_1)^2+(A_0+C_0)^2] +4A_2^2(A_1^2-H_MC_1-A_0C_0)+(H_MC_0-A_0C_1)^2\} \div\{C_0^2+C_1^2+A_1^2+A_2^2\}\,. \quad (1)$$

C_0 and C_1 are functions of θ_B and θ_M such that a focusing condition occurs for which Φ_0 is a minimum. To illustrate this we shall consider the case when both in-pile and detector collimations are relaxed ($A_0, A_2 \to 0$) when equation (1) reduces to

$$F_H^2=k_I^2\frac{A_1^2H_M^2(\cot\theta_B\tan\theta_M)^2}{H_M^2(\cot\theta_B\tan\theta_M-1)^2+A_1^2}, \quad (2)$$

which gives

$$\Phi_0=1/F_H=[(\tan\theta_B\cot\theta_M)^2\eta_M^2 +(1-\tan\theta_B\cot\theta_M)^2\alpha_1^2]^{1/2}\,. \quad (3)$$

The focusing condition then occurs at a value of θ_B such that

$$\tan\theta_B=\tan\theta_M\frac{H_M^2}{H_M^2+A_1^2}=\tan\theta_M\frac{\alpha_1^2}{\alpha_1^2+\eta_M^2} \quad (4)$$

and the observed characteristic width at the focusing position is

$$\Phi_0=\frac{1}{\left(\frac{1}{\eta_M^2}+\frac{1}{\alpha_2^2}\right)^{1/2}}\,. \quad (5)$$

It can be seen from equations (3) and (4) that if the monochromator to sample collimation is also relaxed focusing will occur for $\theta_B=\theta_M$ and that θ_B for focusing will decrease from this value as the collimation (α_1) is decreased. However, if only the detector collimation is relaxed ($A_2 \to 0$) equation (4) becomes

$$\tan\theta_B=\tan\theta_M\frac{H_M^2+2A_0^2}{H_M^2+A_0^2+A_1^2} \quad (6)$$

and it is then possible for focusing to occur at $\theta_B>\theta_M$, when $A_0>A_1$.

It can also be seen from equation (3) that for relaxed in-pile and detector collimations we have $\Phi_0=\eta_M$ when $\theta_B=\theta_M$; *i.e.* the observed peak for an exactly parallel setting under these conditions corresponds directly to the true mosaic of the monochromator. If the collimations are not relaxed we obtain

$$(F_H^2)_{\theta_B=\theta_M}=k_I^2\left\{H_M^2+\frac{4A_1^2(A_0^2+A_2^2)}{A_0^2+A_1^2+A_2^2}\right\}. \quad (7)$$

As we move off the focusing position the collimation becomes increasingly important and the observed width may increase very rapidly at high angles.

(b) Imperfect mosaic sample

If the sample has a finite mosaic spread, then for any angular setting we must integrate the intensity over this mosaic spread.

If the mosaic spread is Gaussian with characteristic angle η_S, and φ_M is the mosaic mis-set angle, then we may consider the scattering cross section to be proportional to $\exp(-\frac{1}{2}\varphi_M^2/\eta_S^2)$, and the intensity is given by

$$I_\varphi=I_0\int_{-\infty}^{+\infty}\exp\{-\tfrac{1}{2}[F_H^2(\varphi+\varphi_M)^2+\varphi_M^2H_S^2k_I^2]\}d\varphi_M, \quad (8)$$

where

$$H_S=1/(\eta_Sk_I)\,. \quad (9)$$

Hence

$$I_\varphi=I_0\frac{\sqrt{2\pi}}{D_M}\exp(-\tfrac{1}{2}F_M^2\varphi^2) \quad (10)$$

and the φ-scan now has a characteristic width of $1/F_M$, where

$$D_M^2=F_H^2+H_S^2k_I^2 \quad (11a)$$

and

$$F_M^2=F_H^2-F_H^4/D_M^2\,. \quad (11b)$$

The observed peak width is then given from equations (11) as

$$\varphi_M=\frac{1}{F_M}=(\Phi_0^2+\eta_S^2)^{1/2} \quad (12)$$

i.e. the observed width is now the square root of the sum of the squares of the width for a perfect sample and the width of the sample mosaic. Equations (1) to (7) are therefore readily extended to allow for the mosaic of the sample. In particular we see that with relaxed in-pile and detector collimation the observed characteristic width is now given by

$$\Phi_M=[(\tan\theta_B\cot\theta_M)^2\eta_M^2 +(1-\tan\theta_B\cot\theta_M)^2\alpha_1^2+\eta_S^2]^{1/2} \quad (13)$$

and in the exact parallel setting this becomes

$$(\Phi_M)_{\theta_B=\theta_M}=(\eta_M^2+\eta_S^2)^{1/2}\,. \quad (14)$$

(c) Integrated intensity

The integrated intensity for a φ-scan is given from equation (10) as

$$I_T=I_0\frac{\sqrt{2\pi}}{D_M}\int_{-\infty}^{+\infty}\exp(-\tfrac{1}{2}F_M^2\varphi^2)d\varphi \quad (15)$$

$$=I_0\frac{2\pi}{D_MF_M}\,. \quad (16)$$

From equation (11) we have

$$D_MF_M=F_HH_Sk_I \quad (17)$$

so that

$$I_T=I_0\frac{2\pi}{F_HH_Sk_I}=I_0\frac{2\pi}{F_H}\eta_S\,. \quad (18)$$

Since in the absence of extinction the integrated intensity must be independent of η_S, we must have that $I_0\propto 1/\eta_S$, and hence $I_T\propto 1/F_H$ as would be expected.

It is in fact more useful to consider the ratio of the integrated intensity to the peak intensity. From equa-

tion (10) we have also that the peak intensity ($\varphi=0$) is $I_P=I_0\sqrt{2\pi}/D_M$.

Hence:

$$I_T=I_P\sqrt{2\pi}/F_M \tag{19}$$

where $1/F_M$ is given by equation (12).

3. θ–2θ scan

(a) Perfect sample

The intensity observed for a θ–2θ scan for a perfect sample has been given in equation (47) of paper III. The characteristic width in $\Delta\theta$ is $1/S_H$ where S_H is defined by equation (46) of paper III.

Expanding the expression for S_H^2 we obtain

$$S_H^2=k_I^2 \times \frac{[A_1^2+A_2^2][(H_M+C_1)^2+(A_0+C_0)^2]+(H_MC_0-A_0C_1)^2}{C_0^2+C_1^2+A_1^2+A_2^2} \tag{20}$$

and the observed width will have a minimum value when

$$\tan\theta_B=\tan\theta_M\,\frac{H_M^2+2A_0^2}{H_M^2+A_0^2+A_1^2+A_2^2}\,. \tag{21}$$

Comparison of equation (20) with equation (1) shows that the only difference in the observed width of a θ–2θ scan and a φ-scan is a term depending on the detector collimation (A_2). Hence, the results given in equations (2) to (6) hold also for a θ–2θ scan, replacing F_H by S_H. However, for $\theta_B=\theta_M$ we must replace equation (7) by

$$(S_H^2)_{\theta_B=\theta_M}=k_I^2\left\{H_M^2+\frac{4A_0^2(A_1^2+A_2^2)}{A_0^2+A_1^2+A_2^2}\right\}. \tag{22}$$

(b) Imperfect mosaic sample

We must again introduce the mosaic spread of the sample as in equation (8). Hence, from equation (41) of paper III we have

$$I_{\varphi,2\theta}=I_0\int_{-\infty}^{+\infty}\exp\{-\tfrac{1}{2}[F_H^2(\varphi+\varphi_M)^2+N^2(\Delta 2\theta)^2 -2(\varphi+\varphi_M)(\Delta 2\theta)L_S+H_S^2k_I^2\varphi_M^2]\}d\varphi_M\,. \tag{23}$$

Hence

$$I_{\theta,2\theta}=I_0\frac{\sqrt{2\pi}}{D_M}\exp\{-\tfrac{1}{2}S_M^2(\Delta\theta)^2\} \tag{24}$$

where

$$S_M^2=S_H^2-(F_H^2-2L_S)^2/D_M^2\,. \tag{25}$$

The peak intensity is thus $I_P=I_0\sqrt{2\pi}/D_M$ as before, and the ratio of the integrated intensity to the peak intensity is

$$I_T/I_P=\sqrt{2\pi}/S_M\,. \tag{26}$$

Again, S_M^2 differs from F_M^2 only in terms depending on the detector collimation (A_2) and if this is relaxed the considerations of § 2(*b*) apply to θ–2θ scans also, replacing F_M by S_M. However, if the detector collimation is not relaxed the expression for the scan widths no longer simplifies readily. It is clear, therefore, that φ-scans are more simple to apply to the determination of sample mosaic, although equation (25) can always be used to predict the width of a particular θ–2θ scan.

4. Experimental measurements

Experimental measurements were made to check some of the expressions derived in § 2 for φ-scan widths. Initially perfect germanium crystals were used as both monochromator and sample, *i.e.* $\eta_M=\eta_S=0$, in order to test the dependence of the observed width on the collimation at various Bragg angles. Further measurements were then made with a copper monochromator ($\eta=0{\cdot}23°$ full-width at half-height) and a perfect germanium sample to test the combined dependence of the observed width on monochromator mosaic and collimation, at various scattering angles, using several values of the detector collimation. The dimensions of these crystals were large compared with the separation of the Soller slits.

The observed half-widths (full-widths at half-height) are listed in Table 1 together with the values calculated from equation (1) using instrumental parameters based on estimates made from the dimensions of the collimators. The agreement obtained is quite satisfactory although no rigorous refinement of these parameters has been made and it is probable that more precise agreement could be achieved if this were done.

The detailed profile of the observed peaks obtained with the two germanium crystals is shown in Fig. 1 as relative intensity as a function of the fractional half-width, *i.e.* all curves have been normalized at the peak position and at the half-width. The solid curve is the average relative intensity and the error bars indicate the

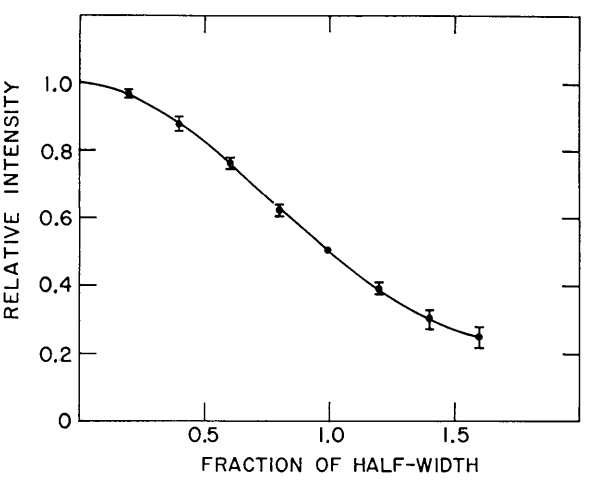

Fig. 1. Relative intensity as a function of the scan range, normalized to the half-width, for observed reflexions using two germanium crystals.

Table 1. *Observed and predicted half-widths of Bragg reflexions*

Monochromator	α_2	h	k	l	Half-width Observed	Calculated
Germanium	4·8°	1	1	1	0·12±0·01°	0·13°
($\eta<0·2'$)		2	2	0	<0·005	—
		4	0	0	0·14±0·01	0·16
		4	4	0	0·40±0·02	0·40
		4	4	4	0·63±0·02	0·54
		8	0	0	0·91±0·03	0·87
Copper	0·35°	1	1	1	0·19±0·01	0·19
($\eta=0·23°$)		2	2	0	0·18±0·01	0·18
		4	0	0	0·17±0·01	0·19
		4	4	0	0·20±0·01	0·21
		4	4	4	0·22±0·01	0·22
		8	0	0	0·23±0·01	0·22
	0·7°	1	1	1	0·20±0·01	0·19
		2	2	0	0·19±0·01	0·20
		4	0	0	0·24±0·01	0·26
		4	4	0	0·31±0·02	0·33
		4	4	4	0·37±0·02	0·37
		8	0	0	0·39±0·02	0·39
	1·4°	1	1	1	0·21±0·01	0·19
		2	2	0	0·20±0·01	0·21
		4	0	0	0·28±0·01	0·31
		4	4	0	0·44±0·02	0·48
		4	4	4	0·57±0·02	0·60
		8	0	0	0·68±0·02	0·68
	4·8°	1	1	1	0·20±0·01	0·19
		2	2	0	0·21±0·01	0·22
		4	0	0	0·33±0·02	0·34
		4	4	0	0·55±0·02	0·59
		4	4	4	0·83±0·03	0·85
		8	0	0	1·13±0·04	1·11

maximum divergence from this curve at intervals of one fifth of the half-width. It can be seen that although the line shape is not exactly Gaussian due to some excess transmission through the elements of the collimators used, it does remain constant over the large range of scattering angles considered.

5. Discussion

The considerations of the previous sections are relevant to both the experimental determination of mosaic spread in imperfect crystals and to the occurrence of focusing effects which are important in the measurement of both Bragg reflexions and diffuse scattering. We have shown that focusing occurs as a function of $2\theta_B$ for both φ and θ–2θ scans and that the width of a particular scan can be predicted from the parameters of the instrument.

There is a growing use of automatic two-crystal diffractometers for the measurement of a relatively large number of Bragg reflexions from a given crystal and in order to use such an instrument efficiently it is important to optimize as far as possible the conditions under which each individual reflexion is measured. This necessarily includes limiting the range of scan over which the measurement is made so that the amount of unwanted background radiation which is measured during the main peak scan is reduced as far as possible. A consideration of the variation of Bragg peak-widths with scattering angle (2θ) is essential and the prediction of focusing conditions and of peak widths as a function of angle may therefore be extremely useful, since the amount of preliminary work on the experimental study of these effects can then be considerably reduced.

In many routine problems a large number of Bragg intensity data of low accuracy are required. In this case a measurement of peak intensity only may be sufficient, provided that this can be related directly to the corresponding integrated intensity. For a well characterized system the relation between the peak and integrated intensities can be calculated by using equation (19) or (26). It is of interest to note that Chidambaram, Sequeira & Sikka (1964) have used this technique successfully using a I_T/I_P curve determined experimentally from some of the strong and medium-strong reflexions.

References

COOPER, M. J. & NATHANS, R. (1968). *Acta Cryst.* A**24**, 619.
CHIDAMBARAM, R., SEQUEIRA, A. S. & SIKKA, S. K. (1964). *Nucl. Instr. and Methods*, **26**, 340.